

# Pairwise controllability and motion primitives for micro-rotors in a bounded Stokes flow

Jake Buzhardt · Vitaliy Fedonyuk · Phanindra Tallapragada

Received: date / Accepted: date

**Abstract** *Micro-robots that can propel themselves in a low Reynolds number fluid flow by converting their rotational motion into translation have begun attracting much attention due to their ease of fabrication. The dynamics and controllability of the motion of such microswimmers are investigated in this paper. The microswimmers under consideration here are spinning spheres (or rotors) whose dynamics are approximated by rotlets, a singularity solution of the Stokes equations. While singularities of Stokes flows are commonly used as theoretical models for microswimmers and micro-robots, rotlet models of microswimmers have received less attention. While a rotlet alone cannot generate translation, a pair of rotlets can interact and execute net motion. Taking the control inputs to be strengths of the micro rotors, the positions of a pair of such rotors are not controllable in an unbounded planar fluid domain. However, in a bounded domain, which is often the case of practical interest, we show that the positions of the micro rotors are controllable. This is enabled by the interaction of the rotors with the boundaries of the domain. We show how control inputs can be constructed based on combinations of Lie brackets to move the rotors*

*from one point to another in the domain. Another contribution of this paper is the creation of a framework for path planning and control of the motion of Stokes singularities that model the dynamics of microswimmers. This can be extended to microswimmers with other shapes moving in confined fluid domains with complex boundaries.*

**Keywords** Micro-robot · Controllability · Motion Planning

## 1 Introduction

The ability to precisely maneuver a micro-robot or a collection of small robots in a small scale fluid environment has enormous implications for areas such as targeted drug delivery [1–4], particle and cell manipulation [2–5], cell identification and diagnostics [6], and the fabrication of novel materials with tunable properties [7]. In recent years, magnetic microswimmers actuated by means of a time-varying external magnetic field have attracted much attention. This is due to the feasibility of fabrication of such robots and the numerous potential applications for remotely controlled locomotion [8–13].

The fabrication of a magnetic swimmer with a specialized geometry is necessary because of the reversibility of flow at low Reynolds numbers [14]. In general, the actuation of a magnetic micro-robot

---

J. Buzhardt · V. Fedonyuk · P. Tallapragada  
Department of Mechanical Engineering  
Clemson University, Clemson, S.C., U.S.A  
Tel.: +1-864-656-5643  
E-mail: ptallap@clemson.edu

could be in the form of a force or a torque, but a net force that directly leads to a translation of the robot requires large gradient of the magnetic field. On the other hand, a torque can be efficiently exerted on the magnetic body via a time-varying magnetic field. Such a torque causes the body to rotate. For bodies possessing the necessary asymmetries, the interaction of the spinning body with the viscous fluid produces a propulsive force [15, 16]. Inspired by the flagellar propulsion of microorganisms, microrobot geometries with helicoidal symmetry are commonly used to achieve this sort of locomotion [3, 5]. More recently, spherical microbeads have been used to construct simpler chiral geometries possessing two perpendicular planes of symmetry but not three [11, 12]. These structures may be fabricated by simpler processes and have been shown to swim theoretically and experimentally. Bodies with spherical or ellipsoidal symmetry, however, do not enable the coupling of a translational motion to a torque, and thus do not translate due to a rotating magnetic field in the absence of a boundary.

While these simple geometries are not able to achieve locomotion in free space, the presence of a boundary can introduce the necessary asymmetry required for translational motion [17, 18]. Even for swimmers that can achieve propulsion in free space, the presence of a boundary can lead to interesting dynamics [19, 20]. The motion of microswimmers with complex geometries is frequently modeled in free space by constructing resistance and mobility matrices that linearly relate the body velocities to the forces and torques exerted on the body. However, this approach is significantly complicated by the presence of no-slip boundaries, as the mobility relationships become dependent on the the position and orientation of the body relative to the boundary. For this reason, singularity models for swimming bodies have become commonplace, as they allow for a rapid approximation of the full fluid velocity field [20, 21]. Furthermore, image systems for these singularity models have been derived to account for the reflected velocity field due to simple boundaries [22].

While a single spinning sphere does not translate in an unbounded domain, two or more closely

spaced spheres can interact hydrodynamically and swim together, essentially tugging each other. Such pair swimmers with very simple geometries do not require any additional fabrication and can replace a single micro-robot with a complex geometry. The mathematical models of the hydrodynamic interactions for such simple bodies are also sufficiently tractable to allow the design of controllers that can control the motion of a pair of such bodies. Pairs of such microrotors could potentially perform manipulation tasks that would otherwise require microrobots with more complex geometries and fabrication procedures.

In this paper, we consider the problem of controlling the motion of two spinning microrotors in a confined domain. We consider a well known approximation of a spinning sphere by a two dimensional rotlet, a singularity of the Stokes equation [16, 23–25]. The velocity field due to a spinning sphere confined to a cross-sectional plane whose normal vector is aligned with the axis of rotation and which passes through the center of the sphere can be approximated by a two-dimensional rotlet [25]. Such a model is appropriate for neutrally buoyant spheres that are constrained by some mechanism, such as a viscous film [26, 27]. Similar two-dimensional models have also been applied to systems of rotating disks [28]. The control inputs for our system are taken to be the strengths of the rotlets, which are directly proportional to the torques on the spheres due to the external magnetic field. We show that the motion of a pair of microrotors in an unbounded domain lacks is not fully controllable due to the existence of an invariant of motion. However in the more practically relevant case of a fluid confined to a bounded domain, the motion of the rotors can be controllable almost everywhere in the domain. We show this through the application of Lie algebra rank condition (LARC), [29–32]. This approach shows the necessary Lie brackets of the control vector fields that allow for motion in any direction of the configuration space of the system of micro rotors. This is illustrated through the computation of a few elementary motions.

While the results in the paper pertain to the case where the micro rotors are confined to a cir-

cular domain of the fluid, the result can be generalized to other bounded geometries of the fluid domain, through the method of conformally mapping a circle to a simply connected region in the complex plane. More importantly, this framework of modeling micro-robots by a few singularities and using this model to control the robots through the motion primitives can be extended to other swimmers such as the helical swimmer and the three-sphere swimmers.

## 2 Dynamics of a pair of micro rotors

The Stokes equations describing the motion of a fluid at a scale where inertial forces are negligible and viscous forces dominate are

$$\nabla p - \mu \nabla^2 \mathbf{u} = \mathbf{0} \quad (1)$$

$$\nabla \cdot \mathbf{u} = 0$$

subject to boundary conditions, where  $\mathbf{u}$  is the velocity of the fluid,  $p$  is the pressure, and  $\mu$  is the dynamic viscosity of the fluid. Singularity solutions of the Stokes equations and linear combinations of such solutions have served as popular models for locomotion [20, 21, 33]. The rotlet is a singularity that describes the velocity of the fluid due to a torque exerted on it at a point, such as due to the spin of the sphere [23].

### 2.1 Rotlets in the Unbounded Domain $\mathbb{R}^2$

The velocity of the fluid at a point  $\mathbf{x} \in \mathbb{R}^2$  due to a rotlet of strength  $\gamma \hat{k}$  located at  $\mathbf{x}_0$  is given by

$$\mathbf{u}(\mathbf{x}) = -\gamma \hat{k} \times \frac{\mathbf{x} - \mathbf{x}_0}{\|\mathbf{x} - \mathbf{x}_0\|^2}. \quad (2)$$

where  $\hat{k}$  is the unit vector orthogonal to the plane of motion.

The stream lines induced by the rotlet form concentric circles around the rotlet, with the speed of the fluid along these streamlines decreasing with the distance from the rotlet. In (2), the velocity  $\mathbf{u}(\mathbf{x})$  becomes undefined at  $\mathbf{x} = \mathbf{x}_0$ . This singularity manifests itself only in the tangential component of the fluid along the streamlines. That is,

in the limit of  $\mathbf{x} = \mathbf{x}_0$ , a fluid particle collocated with the rotlet spins in place but does not move. This motivates one to consider only the desingularized component of the velocity field by assuming that the rotlet does not have a self-induced velocity [16, 25]. Therefore a single rotlet does not move.

If  $n$  rotlets are present in the domain, with the rotlet locations being  $(\mathbf{x}_1, \dots, \mathbf{x}_n)$ , then each rotlet is advected by the velocity field induced by the other  $n - 1$  rotlets. The velocity components of the  $i$ -th rotlet are given by

$$\frac{dx_i}{dt} = \sum_{\substack{j=1 \\ j \neq i}}^n \gamma_j \frac{(y_i - y_j)}{r_{ij}^2} \quad (3)$$

$$\frac{dy_i}{dt} = \sum_{\substack{j=1 \\ j \neq i}}^n -\gamma_j \frac{(x_i - x_j)}{r_{ij}^2}$$

where  $r_{ij} = \sqrt{(x_i - x_j)^2 + (y_i - y_j)^2}$  is the distance between the  $i$ -th and the  $j$ -th rotlets.

Note that while the velocity of the fluid described by (2) is not continuous at the locations of the rotlets, the dynamics of the rotlets themselves are governed by  $C^\infty$  vector fields.

We will consider the specific case of the motion of two rotlets with the control inputs being the strengths of the rotlets,  $\gamma_1$  and  $\gamma_2$ . Equation (3) defines a driftless control affine system, where the positions of the rotlets,  $\xi = [x_1, y_1, x_2, y_2]^T$  evolve on the configuration manifold  $\mathbb{R}^4$ .

We show that regardless of the rotlet strengths, the distance between the rotlets remains invariant. This is seen through a direct calculation. Suppose  $r$  denotes the distance between the two rotlets

$$\begin{aligned} \frac{d}{dt} r^2 &= \frac{d}{dt} ((x_2 - x_1)^2 + (y_2 - y_1)^2) \\ &= 2(x_2 - x_1)(\dot{x}_2 - \dot{x}_1) + 2(y_2 - y_1)(\dot{y}_2 - \dot{y}_1) \\ &= \frac{2}{r^2} (x_2 - x_1)(\gamma_1(y_2 - y_1) - \gamma_2(y_1 - y_2)) \\ &\quad + \frac{2}{r^2} (y_2 - y_1)(-\gamma_1(x_2 - x_1) + \gamma_2(x_1 - x_2)) \\ &= \frac{2}{r^2} (x_2 - x_1)(\gamma_1 + \gamma_2)(y_2 - y_1) \\ &\quad - \frac{2}{r^2} (x_2 - x_1)(\gamma_1 + \gamma_2)(y_2 - y_1) \\ &= 0. \end{aligned}$$

This implies that the control system (3) is not controllable, since neither rotlet can move relative to the other rotlet along the line joining them.

## 2.2 Confined Domain with Circular Boundary

In [24], Meleshko and Aref have shown that the velocity at a point  $\mathbf{x} = (x, y)$  in a bounded, circular domain due to a single point rotlet of strength  $\gamma$  located at  $x = b, y = 0$  is described by the stream function

$$\begin{aligned} \psi(x, y) &= \psi_1 + \psi_2 \\ &= \frac{\gamma}{2} \ln A(x, y) + \frac{\gamma}{2} \left( \ln \frac{1}{B(x, y)} + \frac{C(x, y)}{B(x, y)} \right) \end{aligned} \quad (4)$$

where,

$$\begin{aligned} A(x, y) &= r^2 - 2bx + b^2 \\ B(x, y) &= a^2 - 2bx + \left( \frac{r^2 b^2}{a^2} \right) \\ C(x, y) &= \left( 1 - \frac{r^2}{a^2} \right) \left( a^2 - \frac{r^2 b^2}{a^2} \right) \end{aligned}$$

Here,  $r = \sqrt{x^2 + y^2}$  and  $a$  is the radius of the circular domain. The stream function

$$\psi_1 = \frac{\gamma}{2} \ln(A(x, y))$$

is the same as for the rotlet in the unbounded domain  $\mathbb{R}^2$  and the stream function

$$\psi_2 = \frac{\gamma}{2} \left( \ln \frac{1}{B(x, y)} + \frac{C(x, y)}{B(x, y)} \right)$$

is due to a system of image singularities placed outside the circular domain. The combined stream function  $\psi$  produces a fluid velocity field that satisfies the boundary condition of zero normal and tangential velocity on the boundary. Differentiating (4) gives the velocity field due to a single rotlet

$$\mathbf{V}(x, y) = \frac{\gamma_1}{2} \begin{bmatrix} \frac{(\frac{B}{A})(BA_y - AB_y)}{B^2} + \frac{BC_y - CB_y}{B^2} \\ -\frac{(\frac{B}{A})(BA_x - AB_x)}{B^2} - \frac{BC_x - CB_x}{B^2} \end{bmatrix} \quad (5)$$

where  $A_x, B_x, C_x$  and  $A_y, B_y, C_y$  denote the partial derivatives of the functions with respect to  $x$  and  $y$  respectively.

The velocity of the fluid at a point  $(x, y)$  due to a rotlet of strength  $\gamma_1$  located at  $(x_1, y_1)$  can be obtained from (4) through a rotation transformation of the coordinates. The fluid velocity field is first computed in a frame of reference such that the rotlet lies at  $(b, 0)$  where  $b = \sqrt{x_1^2 + y_1^2}$  and transformed back to the spatial frame,

$$\mathbf{u}(x, y) = \mathbf{R}^{-1}(\theta_1) \mathbf{V}(x, y) \quad (6)$$

where  $\theta_1 = \arctan(y_1/x_1)$  and  $\mathbf{R}(\theta_1)$  is the rotation matrix,

$$\mathbf{R}(\theta_1) = \begin{pmatrix} \cos \theta_1 & \sin \theta_1 \\ -\sin \theta_1 & \cos \theta_1 \end{pmatrix}.$$

As in the case of the unbounded domain, the velocity of the rotlet is desingularized, i.e. a rotlet does not induce a velocity on itself. However the image singularities do induce a velocity on the rotlet,

$$\begin{bmatrix} \frac{dx_1}{dt} \\ \frac{dy_1}{dt} \end{bmatrix} = \mathbf{R}^{-1}(\theta_1) \frac{\gamma_1}{2} \begin{bmatrix} \frac{-B_y}{B} + \frac{BC_y - CB_y}{B^2} \\ \frac{B_x}{B} - \frac{BC_x - CB_x}{B^2} \end{bmatrix}. \quad (7)$$

It is a straightforward calculation to show that only when one rotlet is present in the circular domain, then according to ((7)),  $\mathbf{u} \cdot \mathbf{x} = 0$ . This shows that the rotlet always moves perpendicular to its position vector and therefore executes motion on a circle. This circular path is independent of the strength of the rotlet, which is the only control input. Therefore the position of the rotor is not controllable when only one is present in the domain.

When  $n$  rotlets are present in the circular domain, the velocity of the  $i$ -th rotlet is the sum of the velocities induced by the other  $n - 1$  rotlets, the image systems of the other  $n - 1$  rotlets and its own image singularities. In particular, the governing equations for the motion of two rotlets of

strengths  $\gamma_1$  and  $\gamma_2$  respectively, in the circular domain are

$$\begin{aligned} \begin{bmatrix} \frac{dx_i}{dt} \\ \frac{dy_i}{dt} \end{bmatrix} &= \mathbf{R}^{-1}(\theta_i) \frac{\gamma_i}{2} \begin{bmatrix} -\frac{B_{iy}}{B_i} + \frac{B_i C_{iy} - C_i B_{iy}}{B_i^2} \\ \frac{B_{ix}}{B_i} - \frac{B_i C_{ix} - C_i B_{ix}}{B_i^2} \end{bmatrix} \\ &+ \sum_{\substack{j=1 \\ j \neq i}}^2 \mathbf{R}^{-1}(\theta_j) \frac{\gamma_j}{2} \mathbf{V}_j(x_i, y_i) \end{aligned} \quad (8)$$

In (8)  $\mathbf{V}_j(x_i, y_i)$  is the velocity induced by the  $j$ -th rotlet on  $i$ -th rotlet. The first term on the right hand side of (8) is the velocity induced by the image system of the  $i$ -th rotlet on the  $i$ -th rotlet. The terms  $B_i$  and  $C_i$  are the same as in (4) except that the location of the rotlet is  $(x_i, y_i)$ .

We illustrate the rich dynamics of micro rotors described in this section, by selecting the case of two rotors. Figure 1(a) shows the streamlines of the fluid, at  $t = 0$ , when two rotors each of unit strength,  $\gamma_1 = \gamma_2 = 1$ , are initially located at  $(x_1, y_1) = (0, 0)$  and  $(x_2, y_2) = (0.5, 0)$ . Figure 1(b)-(d) show the ensuing trajectories of the two rotors. Such dynamics can undergo several transitions as the initial location of the rotors changes, as discussed in [34].

In the rest of the paper, we focus on the motion and controllability of a pair of micro rotors whose governing equations are (8).

### 3 Controllability

The position of the two micro rotors parameterized by  $\xi = [x_1, y_1, x_2, y_2]^T$  evolves on the configuration manifold  $\mathbb{Q} = \{(x_1, y_1, x_2, y_2) \in \mathbb{R}^4 \mid x_1^2 + y_1^2 \leq a^2 \wedge x_2^2 + y_2^2 \leq a^2\}$ . The tangent space at any point  $\xi \in \mathbb{Q}$  will be denoted by  $T_\xi \mathbb{Q}$ . The governing equation (8) for the motion of the rotlets is a driftless control affine system,  $\Sigma$ , with the strengths of the rotlets being the control inputs  $\gamma_1$  and  $\gamma_2$

$$\Sigma: \dot{\xi} = g_1(\xi)\gamma_1 + g_2(\xi)\gamma_2 \quad (9)$$

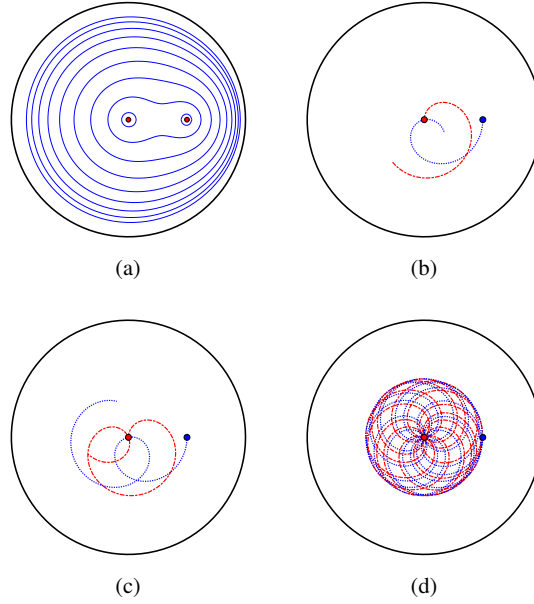


Fig. 1: (a) Streamlines of the fluid when two rotlets of unit strength are located at  $(0, 0)$  and  $(0.5, 0)$ . (b), (c), and (d) show trajectories of the two rotlets,  $(x_1(t), y_1(t))$  and  $(x_2(t), y_2(t))$  for (b)  $0 \leq t \leq 1$ , (c)  $0 \leq t \leq 2$ , and (d)  $0 \leq t \leq 15$ .

where  $g_1$  and  $g_2$  are  $C^\infty$  vector fields and  $\gamma_1 \in \mathbb{R}$  and  $\gamma_2 \in \mathbb{R}$ . Here each of the vector fields  $g_i(\xi)$  is a column vector whose elements are the coefficients of  $\gamma_i$  from (8).

#### 3.1 Small time local controllability

We first show that the two rotlets can move in any direction from almost any initial positions in an arbitrarily small time, i.e. for almost any initial state  $\xi_0$  of the control system  $\Sigma$ , and small enough time  $t_0$ , the reachable set  $R_\Sigma(t < t_0, \xi_0)$  contains a neighborhood of  $\xi_0$ . This is shown using the Lie algebra rank condition (LARC) [29–32].

Given two vector fields,  $g_i$  and  $g_j$  the Lie bracket, denoted  $[g_i, g_j]$  is defined as

$$[g_i, g_j] = \nabla g_j g_i - \nabla g_i g_j.$$

This Lie bracket can be interpreted as the infinitesimal motion that results from flowing in the sequence of directions  $g_i, g_j, -g_i, -g_j$ . Associated

with the control system  $\Sigma$  is a distribution

$$\Delta = \text{span}\{g_1, g_2\} \quad (10)$$

whose closure under Lie bracketing we denote by  $\bar{\Delta}$ . For drift free control systems, such as (9), the Lie algebra rank condition states that if  $\xi \in \mathbb{Q}$  and  $\dim(\bar{\Delta}_\xi) = \dim(T_\xi \mathbb{Q})$ , then the system is small time locally controllable (STLC) [29–32]. For drift-free systems such as  $\Sigma$ , small-time local controllability implies controllability [29].

To evaluate the controllability of a system of two rotlets in a confined circular domain, we apply the LARC to (8). The explicit calculation of the Lie brackets of (9), performed using the software Maple, is not shown here to avoid long expressions. Furthermore, deeply nested brackets are difficult to compute even using a software like Maple. The linear independence of the Lie brackets is evaluated numerically at specific values of  $\xi$ . By numerically evaluating a set of Lie brackets for 10,000 different values of  $\xi$  distributed uniformly throughout the domain we find that the vector fields

$$\begin{aligned} &g_1 \\ &g_2 \\ &[g_1, g_2] \\ &[g_1, [g_1, g_2]] \end{aligned} \quad (11)$$

span the tangent space  $T_\xi \mathbb{Q} = \mathbb{R}^4$  at all points  $\xi \in \mathbb{Q}$  except the special configurations in which both rotlets lie on a chord passing through the center of the circular domain. We denote this configuration by  $S$  and express it mathematically as

$$S = \{(x_1, y_1, x_2, y_2) \in \mathbb{Q} \mid \exists \lambda \text{ s.t. } \lambda(x_1, y_1)^T = (x_2, y_2)^T\}$$

Higher order Lie brackets were not evaluated for  $\xi \in S$  since the computations were numerically unstable. The set  $C$  is dense in  $\mathbb{Q}$ . The possible deficiency in the dimension of  $\bar{\Delta}$  for  $\xi \in S$  does not however preclude controllability, but only small time local controllability. This is because for any  $\xi \in S$  the Lie brackets in (11) span the directions perpendicular to the line joining the rotlets. This means that on  $S$  the rotlets can still move parallel to one another such that they enters the set  $C$  and from any initial configuration  $\xi_0 \in C$ , the system

of two rotlets can be driven in any direction in an arbitrarily small amount of time through a motion generated by the Lie brackets given in (11).

#### 4 Simulation of Lie Brackets and Motion Planning

It has been shown above that for most configurations, four linearly independent vector fields from the Lie algebra can be found to span the tangent space. This means that there exist inputs  $\gamma_1$  and  $\gamma_2$  that can produce motion in any desired direction. We show motion along each of the Lie bracket directions by integrating the the vector fields (11) in time. Motion due to each of the vector fields is illustrated in Fig. 2.

The motion of the rotlets associated with the vector field  $g_1$  is merely the motion of a rotlet and a non-spinning sphere or a fluid tracer ( $\gamma_2 = 0$ ). The trajectory of the two rotors for this vector field is shown in Fig. 2(a) for a generic initial position  $\xi_0 \in C$ . Similarly, the motion of the rotlets associated with the vector field  $g_2$  is shown in Fig. 2(b). The motion associated with the vector fields  $[g_1, g_2]$  and  $[g_1, [g_1, g_2]]$  in Fig. 2 is obtained by numerically integrating the equations  $\dot{\xi} = [g_1, g_2]$  and  $\dot{\xi} = [g_1, [g_1, g_2]]$ .

##### 4.1 Motion in a Given Direction

It has been shown that the vector fields given by the Lie brackets in (11) span the tangent space  $T_{\xi_0} \mathbb{Q}$  associated with the system  $\Sigma$  of (9) at any configuration  $\xi_0 \in C$ , and thus  $\Sigma$  is locally controllable from these configurations. Therefore, a motion in the direction of any vector  $v \in T_{\xi_0} \mathbb{Q}$  may be generated by some linear combination of the Lie brackets that span the tangent space. With the Lie brackets given in (11) we can write

$$\begin{aligned} v &= a_1 g_1 + a_2 g_2 + a_3 [g_1, g_2] + a_4 [g_1, [g_1, g_2]] \\ &= G(\xi_0) a \end{aligned} \quad (12)$$

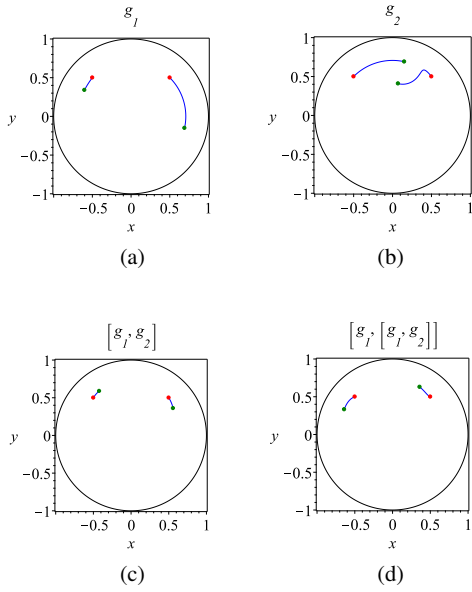


Fig. 2: Rotlet motion due to the vector fields  $g_1$ ,  $g_2$ ,  $[g_1, g_2]$ , and  $[g_1, [g_1, g_2]]$  for 1 time unit from an initial configuration shown by red filled circles at  $\xi(0) = [0.5, 0.5, -0.5, 0.5]^T$ . Green filled circles denote the final positions of the rotlets at  $t = 1$ .

where  $G(\xi_0)$  is the matrix with columns given by the vector fields in (11) evaluated at the initial configuration  $\xi_0$  and  $a$  is a vector of coefficients. While the matrix  $G(\xi_0)$  depends on the initial configuration, it has full rank for any  $\xi_0 \in C$ . Therefore,  $G(\xi_0)$  is invertible and we can solve for the coefficients needed to achieve motion in an arbitrary direction  $v \in T_{\xi_0} \mathbb{Q}$  as

$$a = [G(\xi_0)]^{-1} v \quad (13)$$

Solving this equation yields the linear combination of the vector fields that is required to instantaneously steer the system from a given state  $\xi_0 \in C$  in the direction specified by  $v \in T_{\xi_0} \mathbb{Q}$ .

Equation (13) describes a way to generate a velocity in any arbitrary direction  $v$  from any configuration  $\xi_0 \in C$ . Therefore, this procedure may be used to compute the linear combination of the control vector fields needed to produce the velocity required at each instant for the system to track a

path through the controllable subspace. To demonstrate the controllability of the system and the use of this technique, we show several kinds of simple motions for the system in Fig. 3, along with the coefficients of the vector fields required to generate them. These motions include the following - the two rotors moving along a line a joining each other, towards each other in Fig. 3(a.1) together in Fig. 3(b.1) and moving in a direction perpendicular to the line joining them, in Figs. 3(c.1)-(d.1). The subfigures Fig.3(a.2), (b.2), (c.2) and (d.2) show the variation in the coefficients  $a_1 - a_4$  along the trajectories of the rotors. We note that these coefficients are directly related to the control inputs  $\gamma_1$  and  $\gamma_2$ . The initial condition for the system in all the cases shown in Fig. 3 is the arbitrarily chosen point  $\xi_0 = [0.5, 0, -0.25, 0.25]^T$ .

Prescribed trajectories of the rotors as well as for the case of motion in a formation can be constructed from such primitives. It is plausible that generic smooth curves can also be tracked by the rotors by combining the infinitesimal flows generated by the Lie brackets along a prescribed path using the techniques outlined in [31, 35].

## 5 Conclusion

Stokes flow singularities serve as convenient mathematical approximations of microscale swimmers in a low Reynolds number flow. For instance, rotlets serve as a model for spinning spheres, while a translating sphere is modeled by a Stokeslet with a potential dipole. For more complex geometries, such as flagellar and helical swimmers, the swimmer surface may be discretized into a distribution of singularities in a boundary element formulation. Singularities can also be useful to model the effects of fixed or moving boundaries and the interaction with other swimmers. Singularity models can lead to low dimensional but physically realistic control models of micro swimmers and allow for the formulation of path planning algorithms. Furthermore these models provide an insight into controllability or lack thereof for individual swimmers or for a collection of swimmers.

The above themes have been explored in this paper through an idealized system of two spinning

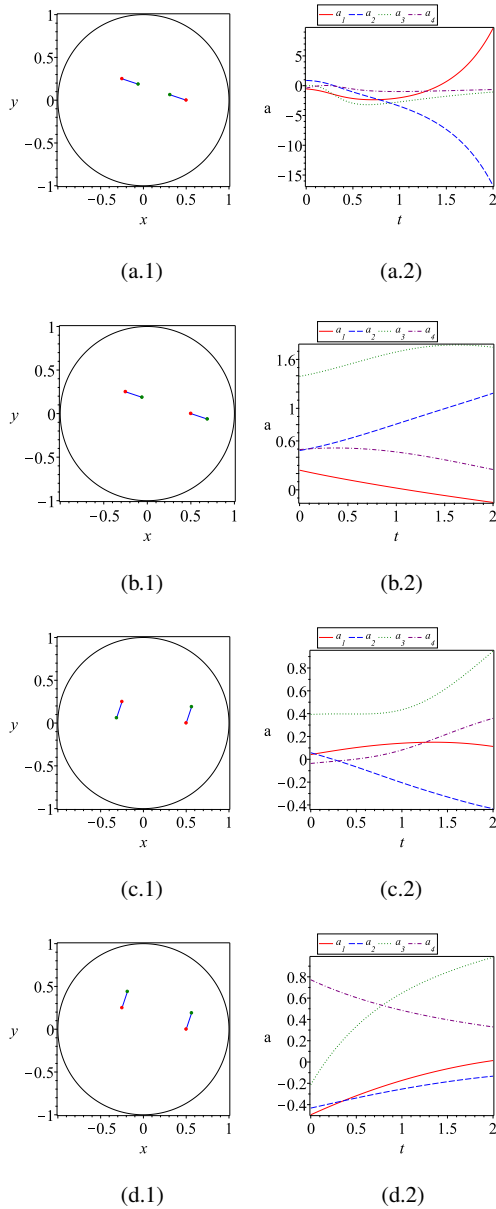


Fig. 3: Demonstration of some elementary pairwise motions of the rotlets. The left hand column shows the simulated trajectories of the rotlets as they move along straight line paths at a constant speed of 0.1 for two time units. The right hand column shows the corresponding combination of of the control vector fields and Lie bracket vector fields required at each instant to achieve this motion. The coefficients  $a_1, a_2, a_3, a_4$  refer to those of Eq. (12), which are directly related to the control inputs.

spheres, approximated by rotlets. A single rotlet cannot generate a translational motion in an unbounded domain and while they can move in a confined domain, such as a circular region, this motion is not controllable. We have shown that due to the existence of an invariant, the motion of a system of two rotlets is uncontrollable in the idealized setting of an unbounded domain. However, through numerical computations and the application of the Lie algebra rank condition, we have shown that a comparable system of two rotlets in a bounded, circular domain is controllable due to the presence of a boundary. This finding implies that spherical microrobots, which are easily fabricated, can move as pairs in a controllable fashion, even though individually they cannot. A pair of such simple robots could perform manipulation tasks that otherwise would require a micro robot with specialized geometry. Furthermore, the model used herein of the rotlet in the presence of a boundary is more representative of a physical system than the idealized model of an unbounded domain.

The results of the path planning framework and motion primitives for Stokes singularities that has been presented in this paper, can be extended to the dynamics and control of the three dimensional motion of realistic microswimmers such as helical swimmers and the three-sphere swimmers [11] whose motion can be approximated by that of a few singularities. Potential future directions of study include control of individual swimmers in complex domains, the development of motion primitives, and their extension to the control of the motion of collections of microswimmers.

## References

1. B. J. Nelson, I. K. Kaliakatsos, and J. J. Abbott. Microrobots for minimally invasive medicine. *Annual Review of Biomedical Engineering*, 12:55–85, 2010.
2. L. Zhang, T. Petit, K. E. Peyer, and B. J. Nelson. Targeted cargo delivery using a rotating nickel nanowire. *Nanomedicine*, 8(7):1074–80, 2012.
3. K. E. Peyer, L. Zhang, and B. J. Nelson. Bio-inspired magnetic swimming microrobots



- for biomedical applications. *Nanoscale*, 4(5):1259–1272, 2013.
4. W. Gao, D. Kagan, C. Clawson, S. Campuzano, E. Chuluun-Erdene, E. Shipton, E. Fullerton, L. Zhang, E. Lauga, and J. Wang. Cargo-towing fuel-free magnetic nanoswimmers for targeted drug delivery. *Small*, 2012.
  5. T. Petit, L. Zhang, K. E. Peyer, B. E. Kratochvil, and B. J. Nelson. Selective trapping and manipulation of microscale objects using mobile microvortices. *Nano Letters*, 12(1):156160, 2012.
  6. Y. Ding, F. Qiu, X. C. Solvas, F. W. Y. Chiu, B. J. Nelson, and A. de Mello. Microfluidic-based droplet and cell manipulations using artificial bacterial flagella. *Micromachines*, 7(2):25, 2016.
  7. A. Snezhko and I. S. Aranson. Magnetic manipulation of self-assembled colloidal asters. *Nature materials*, 10:698–703, 2011.
  8. R. Dreyfus, J. Baudry, M. L. Roper, M. Fermigier, H. A. Stone, and J. Bibette. Microscopic artificial swimmers. *Nature*, 2005.
  9. L. Zhang, J. J. Abbott, L. Dong, B. E. Kratochvil, D. Bell, and B. J. Nelson. Artificial bacterial flagella: Fabrication and magnetic control. *Applied Physics Letters*, 94:064107, 2009.
  10. A. Ghosh, P. Mandal, S. Karmakar, and A. Ghosh. Analytical theory and stability analysis of an elongated nanoscale object under external torque. *Physical Chemistry Chemical Physics*, 15:10817, 2013.
  11. U. K. Cheang, F. Meshkati, D. Kim, M. J. Kim, and H. C. Fu. Minimal geometric requirements for micropropulsion via magnetic rotation. *Physical Review E*, 2014.
  12. F. Meshkati and H. Fu. Modeling rigid magnetically rotated microswimmers: Rotation axes, bistability, and controllability. *Physical Review E*, 90(6):063006, 2014.
  13. X. Z. Chen, M. Hoop, F. Mushtaq, E. Siringil, C. Hu, B. J. Nelson, and S. Pané. Recent developments in magnetically driven micro- and nanorobots. *Applied Materials Today*, 9:37–48, 2017.
  14. E. M. Purcell. Life at low reynolds number. *American Journal of Physics*, 45:3–11, 1977.
  15. J. Happel and H. Brenner. *Low Reynolds number hydrodynamics: with special applications to particulate media (Mechanics of Fluids and Transport Processes)*. Springer, 1983.
  16. S. Kim and S. J. Karrila. *Microhydrodynamics: Principles and Selected Applications*. Dover Publications, 2005.
  17. P. Tierno, R. Golestanian, I. Pagonabarraga, and F. Sagués. Controlled swimming in confined fluids of magnetically actuated colloidal rotors. *Phys. Rev. Lett.*, 101:218304, Nov 2008.
  18. Y. Or, S. Zhang, and R. Murray. Dynamics and stability of low-reynolds-number swimming near a wall. *SIAM Journal on Applied Dynamical Systems*, 10(3):1013–1041, 2011.
  19. E. Lauga, W. R. DiLuzio, G. M. Whitesides, and H. A. Stone. Swimming in circles: Motion of bacteria near solid boundaries. *Biophysical Journal*, 90(2):400 – 412, 2006.
  20. S.E. Spagnolie and E. Lauga. Hydrodynamics of self-propulsion near a boundary: predictions and accuracy of far-field approximations. *Journal of Fluid Mechanics*, 700:105147, 2012.
  21. A.T. Chwang and T.Y. Wu. Hydromechanics of low-reynolds-number flow. part 2. singularity method for stokes flows. *Journal of Fluid Mechanics*, 67(4):787815, 1975.
  22. J. R. Blake and A. T. Chwang. Fundamental singularities of viscous flow. *Journal of Engineering Mathematics*, 8(1):23–29, Jan 1974.
  23. G. K. Batchelor. The stress system in a suspension of force-free particles. *Journal of Fluid Mechanics*, 41(3):545570, 1970.
  24. V. V. Meleshko and H. Aref. A blinking rotlet model for chaotic advection. *Physics of Fluids*, (8):3215, 1996.
  25. E. Lushi and P. M. Vlahovska. Periodic and chaotic orbits of plane-confined micro-rotors in creeping flows. *Journal of Nonlinear Science*, 25(5):11111123, 2015.
  26. M. Leoni and T. B. Liverpool. Dynamics and interactions of active rotors. *EPL (Europhysics Letters)*, 92(6):64004, 2010.

27. Y. Fily, A. Baskaran, and M.C. Marchetti. Co-operative self-propulsion of active and passive rotors. *Soft Matter*, 8:3002–3009, 2012.
28. B. A. Grzybowski, H.A. Stone, and G.M. Whitesides. Dynamics of self assembly of magnetized disks rotating at the liquid–air interface. *PNAS*, 99(7):4147–4151, 2002.
29. R. Murray, Z. Li, and S. S. Sastry. *A Mathematical Introduction to Robotic Manipulation*. CRC Press, 1994.
30. S. Sastry. *Nonlinear Systems: Analysis, Stability, and Control*. Springer Verlag-Berlin, 1999.
31. F. Bullo and A. D. Lewis. *Geometric Control of Mechanical Systems*. Springer Verlag-Berlin, 2004.
32. A. M. Bloch. *Nonholonomic Mechanics and Control*. Springer Verlag, 2003.
33. E. Lauga and Powers. The hydrodynamics of swimming microorganisms. *Reports on Progress in Physics*, 72(9):096601, 2009.
34. S. Sudarsanam and P. Tallapragada. Chaotic mixing using micro-rotors in a confined domain. *Submitted to Physics of Fluids*, 2018.
35. S. Kadam, K. Joshi, N. Gupta, P. Katdare, and R. Banavar. Trajectory tracking using motion primitives for the purcell’s swimmer. In *2017 IEEE/RSJ International Conference on Intelligent Robots and Systems (IROS)*, pages 3246–3251, Sept 2017.